A New Series of ZnII Coordination Polymer Based Metallogels Derived from Bis-pyridyl-bis-amide Ligands: A Crystal Engineering Approach

ARTICLE *in* CRYSTAL GROWTH & DESIGN · DECEMBER 2010

Impact Factor: 4.89 · DOI: 10.1021/cg101342g

2 AUTHORS, INCLUDING:

Nayarassery Narayanan Adarsh
Catalan Institute of Nanoscience and Nanot…

46 PUBLICATIONS **762** CITATIONS

SEE PROFILE

DOI: 10.1021/cg101342g

CRYSTAL GROWTH & DESIGN Article

2011, Vol. 11
328–336

Published as part of a virtual special issue on Structural Chemistry in India: Emerging Themes.

A New Series of Zn^{II} Coordination Polymer Based Metallogels Derived from Bis-pyridyl-bis-amide Ligands: A Crystal Engineering Approach

N. N. Adarsh and Parthasarathi Dastidar*

Department of Organic Chemistry, Indian Association for the Cultivation of Science (IACS), 2A&2B, Raja S. C. Mullick Road, Jadavpur, Kolkata − 700032, West Bengal, India

Received October 12, 2010; Revised Manuscript Received November 6, 2010

ABSTRACT: On the basis of a recently demonstrated crystal engineering strategy, two hydrogen bond equipped bidentate ligands, namely, *N,N′*-bis-(3-pyridyl)isophthalamide **L1** and *N,N′*-bis-(3-pyridyl)terephthalamide **L2**, have been exploited to generate a new series of Zn^{II}-coordination polymer based metallogels. As many as 12 metallogels have been prepared by the reaction of these ligands with various Zn^{II} halides under various conditions. The gels were characterized by rheology, scanning electron microscopy (SEM), and powder X-ray diffraction (PXRD). A structure−property correlation study based on the PXRD of the xerogels and single crystal X-ray diffraction (SXRD) data of some of the isolated single crystals of the reaction products clearly establishes the structures of the gel fibers in the xerogels and supports the crystal engineering based design strategy based on which metallogels are prepared.

Introduction

Gels are commonplace in and around us. Anyone who has experienced "sheer-thinning" by squirting it through the teeth while eating a gelatinous desert knows what a gel state is.[1] A gel is comprised of mainly a small amount of gelator and a large volume of liquid. Typically, a gel is formed when a solution containing a critical concentration of gelator (minimum gelator concentration or MGC) is heated and cooled below a critical temperature (sol−gel transition temperature). If the whole volume of the liquid is able to withstand its own weight under the gravitational force (usually tested by tube inversion), it is called a gel. It is widely believed that the solvent molecules are immobilized due to capillary force action within the gel network either formed via covalent bond formation (chemical gel) or supramolecular self-assembly (physical or supramolecular gel).[2] Metallogels[3] are soft materials wherein metal atoms play a significant role in forming the gel network.[4] Discrete metal coordination complexes,[5] well-defined coordination polymers,[6] or cross-linked coordination polymers[7] are all known to act as metallogels. Other classes of gel systems containing metals are also known; noncoordinating metal ions or metal nanoparticles incorporated in the gel matrix are shown to act as growth regulators for the preparation of metallic nanoparticles or as templates for the formation of porous or nanoimprinted supramolecular assemblies.[8] The morphology and kinetics of gel formation[9] have also been shown to be dependent on the presence of metal ions in the gel matrix.

Research on metallogels is increasingly becoming important as they offer potential applications in catalysis,[10a] sensing,[10b] optics,[10c] magnetic materials,[10d] etc. Designing a metallo-gelator is a daunting task. Nevertheless, there have been some attempts to design metallogelators: appending aromatic-linker-steroid (ALS) (well-known gel forming fragment) to an organo-metallic moiety,[11a] introducing long alkyl chain on coordination complex,[11b] aborting crystallization by increasing the randomness of mixed ligand carboxylates of Ag^{I} coordination compounds,[11c] flexible ligand coordination and slow formation of coordination polymers,[11d] and supramolecular synthon approaches[11e] are a few examples of metallogelators obtained by design.

The present study concerns an alternative design strategy; it may be noted that both gels and solvent occluded crystalline solids have one thing in common; that is, in both the cases, large quantities of solvent molecules are trapped within the corresponding networks that are formed by supramolecular assembly of molecules. We[12] and others[13] have shown that the single crystal structures of some gelator molecules capable of gelling highly polar solvents or mixture of solvents such as DMSO, DMF, water, ethylene glycol, and their various mixtures contain a large amount of lattice occluded solvents. Thus, coordination compounds having structural features of inducing both gelation and formation of lattice occluded crystalline solids may be good targets as metallogelators. Following this design strategy, in a recent study, we have been able to synthesize a series of metallogelators derived from mixed ligand systems involving bis-pyridyl-bis-amide ligands **L1** and **L2**, various dicarboxylates, and Cu^{II}/Co^{II} salts.[14] Encouraged by these results, we have decided to exploit these two positional isomeric ligands **L1** and **L2** further to generate new metallogelators. The hydrogen bonding backbone, conformational flexibility, and conformation-dependent ligating topology make these ligands especially attractive as the corresponding coordination compounds when reacted with a suitable metal salt displayed variety of supramolecular structures

*To whom correspondence should be addressed. E-mail: parthod123@rediffmail.com; ocpd@iacs.res.in.

 Published on Web 12/03/2010

Scheme 1

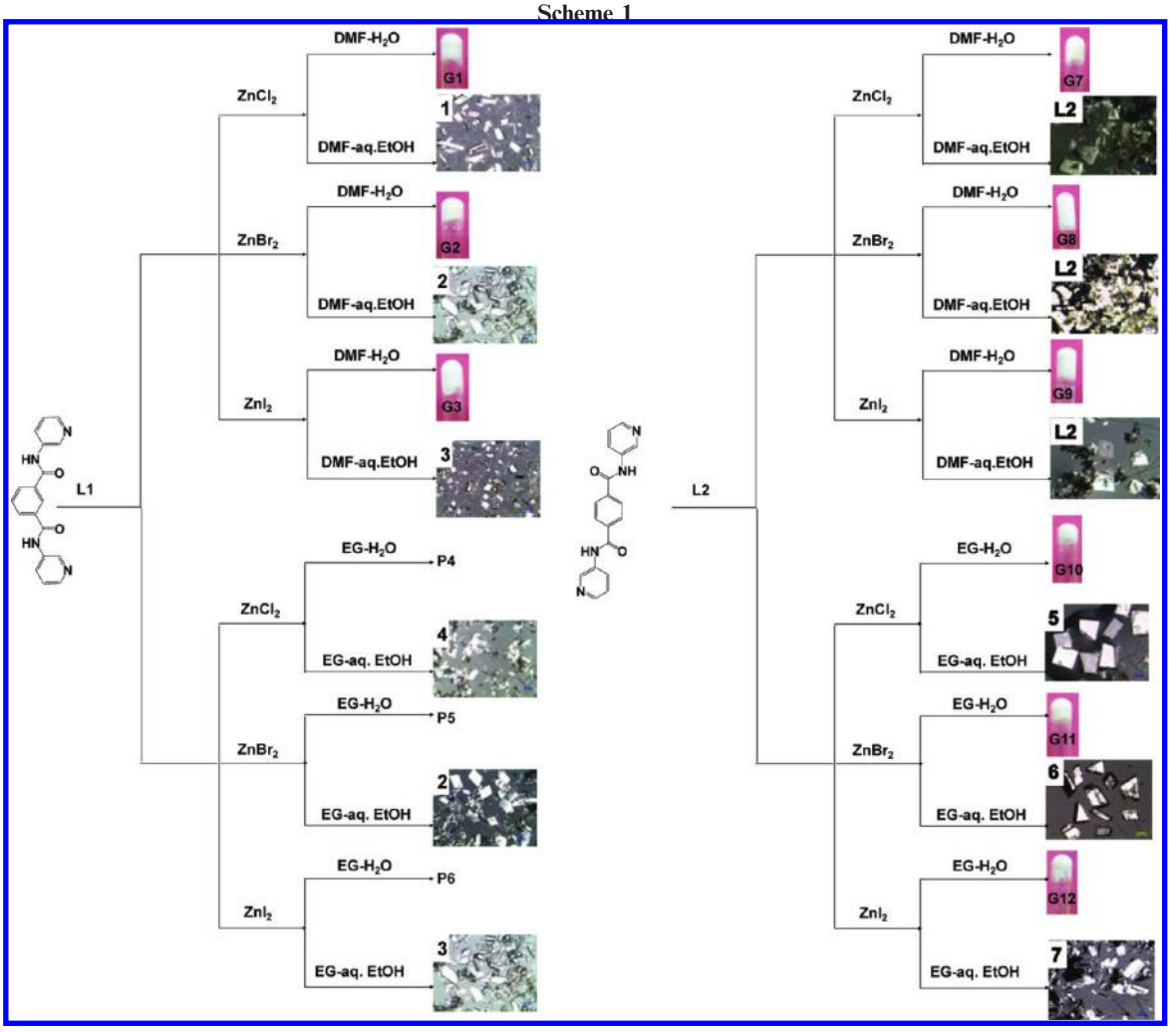

Table 1. Gelation Data[a]

gel	metal salt	pyridyl ligand	solvent	minimum gelator concentration (MGC) (wt %)
G1	$ZnCl_2$ (12.8 mg, 0.094 mmol)	**L1** (30 mg, 0.094 mmol)	DMF/H_2O (3:7, v/v)	4.3
G2	$ZnBr_2$ (21 mg, 0.094 mmol)	**L1** (30 mg, 0.094 mmol)	DMF/H_2O (3:7, v/v)	5.1
G3	ZnI_2 (30 mg, 0.094 mmol)	**L1** (30 mg, 0.094 mmol)	DMF/H_2O (3:7, v/v)	6.0
G7	$ZnCl_2$ (21.7 mg, 0.16 mmol)	**L2** (50 mg, 0.16 mmol)	DMF/H_2O (3:7, v/v)	7.2
G8	$ZnBr_2$ (35.6 mg, 0.16 mmol)	**L2** (50 mg, 0.16 mmol)	DMF/H_2O (3:7, v/v)	8.6
G9	ZnI_2 (51 mg, 0.25 mmol)	**L2** (50 mg, 0.16 mmol)	DMF/H_2O (3:7, v/v)	10.0
G10	$ZnCl_2$ (12.8 mg, 0.094 mmol)	**L2** (30 mg, 0.094 mmol)	EG/H_2O (3:7, v/v)	4.3
G11	$ZnBr_2$ (21 mg, 0.094 mmol)	**L2** (30 mg, 0.094 mmol)	EG/H_2O (3:7, v/v)	5.1
G12	ZnI_2 (30 mg, 0.094 mmol)	**L2** (30 mg, 0.094 mmol)	EG/H_2O (3:7, v/v)	6.0

[a] Microscopic observation of the xerogels under a field scanning electron microscope (FE-SEM) revealed the presence of a typical fibrous network in all the cases except **G7**−**G9** wherein flake-type morphology was observed (Figure 1). Understandably, the solvent molecules were immobilized within the network resulting in gel formation.

and properties.[15] While **L1** can display both metallamacrocycle[16a] and helix,[16b] the positional isomer **L2** is shown to produce mainly one-dimensional (1-D) zigzag coordination polymers[16c] when they were reacted with metal salts in a 1:1 molar ratio. These ligands owing to their conformational flexibility and hydrogen bonding backbone may occlude solvent molecules in the crystal lattice of the corresponding coordination compounds in the presence of suitable solvent system. Thus, 1:1 (metal/ligand) coordination compounds derived from **L1** and **L2** are expected to show metallogelation properties under suitable conditions. In this article, we report the synthesis and single crystal X-ray diffraction (SXRD) structures of a few 1:1 (metal/ligand) coordination compounds derived from these two ligands and Zn^{II} halides. Some of the coordination compounds indeed form metallogels which are characterized by various physicochemical techniques such as rheology, scanning electron microscopy (SEM), powder X-ray diffraction (PXRD), etc. Structures of the some of the gel networks in their xerogel forms are also elucidated by comparing PXRD and SXRD data.

Results and Discussion

Thus, we have reacted both the ligands in separate experiments with various Zn^{II} halides in a 1:1 (metal/ligand) molar ratio. The reason for choosing Zn^{II} halides is because of the

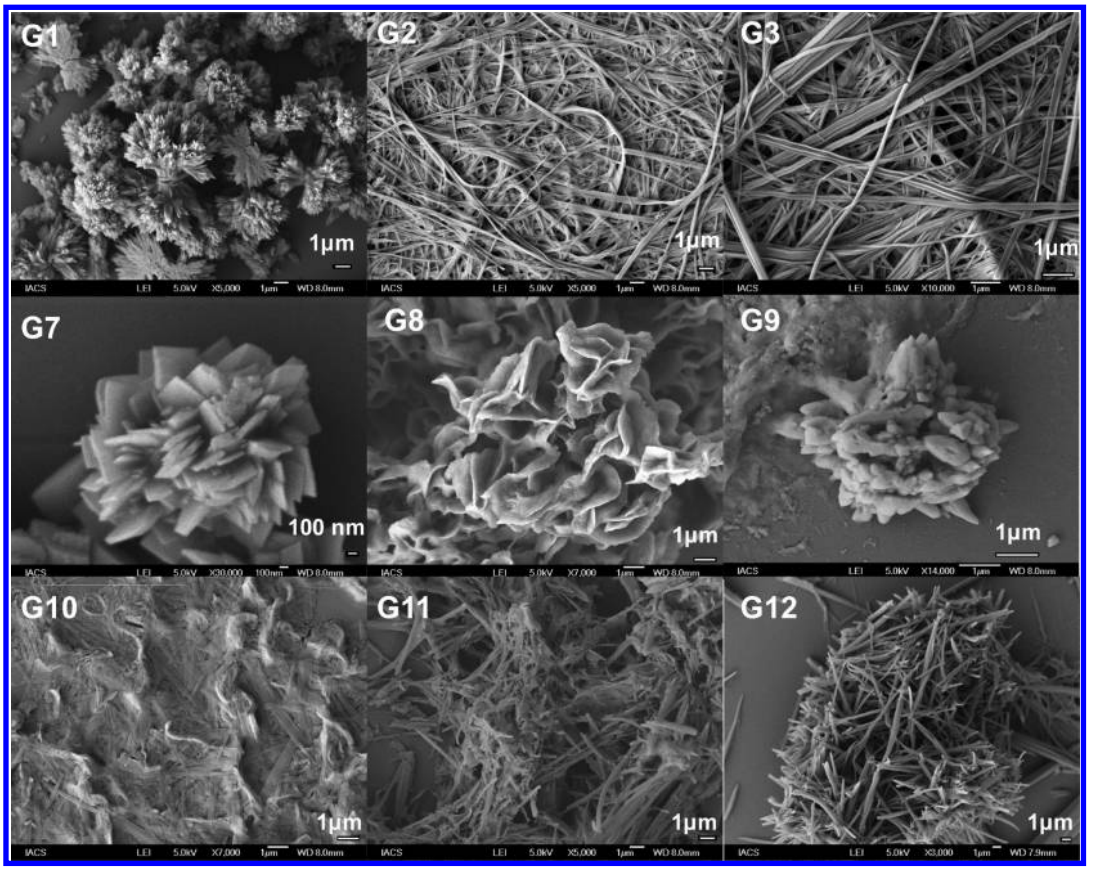

Figure 1. FE-SEM micrographs of the typical fibrous networks of **G1**−**G3** and **G7**−**G12**.

fact that halides are generally strongly coordinated to a Zn^{II} metal center ensuring the formation of 1:1 (metal/ligand) coordination compounds.[17] It has been found that while **L1** could gel a DMF/water (3:7, v/v) mixture, **L2** could solidify both DMF/water (3:7, v/v) and ethylene glycol (EG)/water (3:7, v/v) when they were reacted with different Zn^{II} halides ($ZnCl_2$, $ZnBr_2$, and ZnI_2) in a sonication bath (Scheme 1); the overall concentration of 4−10 wt % (w/v) (considering all the reactants) and a brief sonication were required to effect gelation (Table 1). The gels were not thermo-reversible indicating the coordination polymeric nature of the gel network; the gels were stable under ambient conditions for more than a week.

To characterize the gels further, the rheological response using dynamic rheology was tested for some selected gels. All these gels studied for rheology displayed typical gel-like rheological response wherein the elastic modulus G′ was found to be independent of frequency and considerably higher than the loss modulus G″ over the range of frequencies (Figure 2). Thus, tube inversion, SEM, and rheology data clearly indicated that **G1**−**G3** and **G7**−**G12** were indeed gels.

It is now important to establish the structures of the gelling agents which might deliver new insights into the designing aspects based on where the present study began; it is understandable that it is virtually not possible to determine the single crystal structure of a gel fiber which is too tiny to collect single crystal X-ray diffraction data. The other alternative approach wherein the structure of a gel network is determined ab intio[18] by PXRD is not yet a routine method and often suffers from poor data set due to the scattering contribution of the solvent molecules as well as the less crystalline nature of

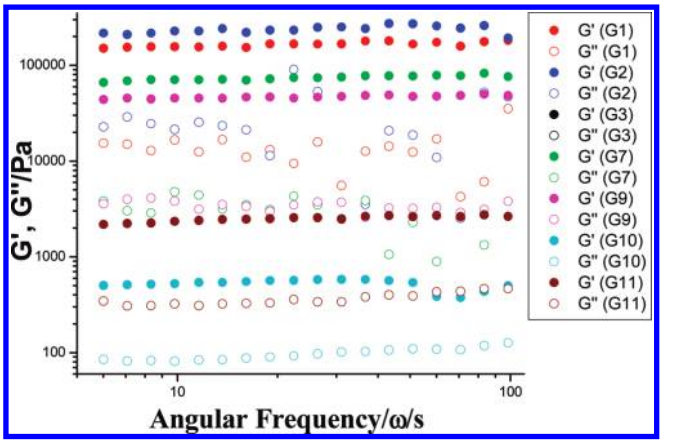

Figure 2. Rheological response of some of the selected gels.

the gel fibers requiring high intensity X-ray source such as the not-so-easily accessible synchrotron beamline. On the other hand, the structure of a gel network can be determined by comparing PXRD of the xerogel with that obtained by simulating the single crystal data of the gelator. This type of indirect approach is found to be effective, although there is no certainty that crystal structure of a gel fiber in its xerogel state truly represents that in a gelled state.[19] A reasonable match of the PXRD of the xerogel with that of simulated one indirectly establishes the structure of the gel fiber in a xerogel.[20] With this background, we tried to crystallize all the coordination compounds as depicted in Scheme 1.

Thus, we tried to get the thermodynamically more stable neat single crystals of the gelling agents by reacting the

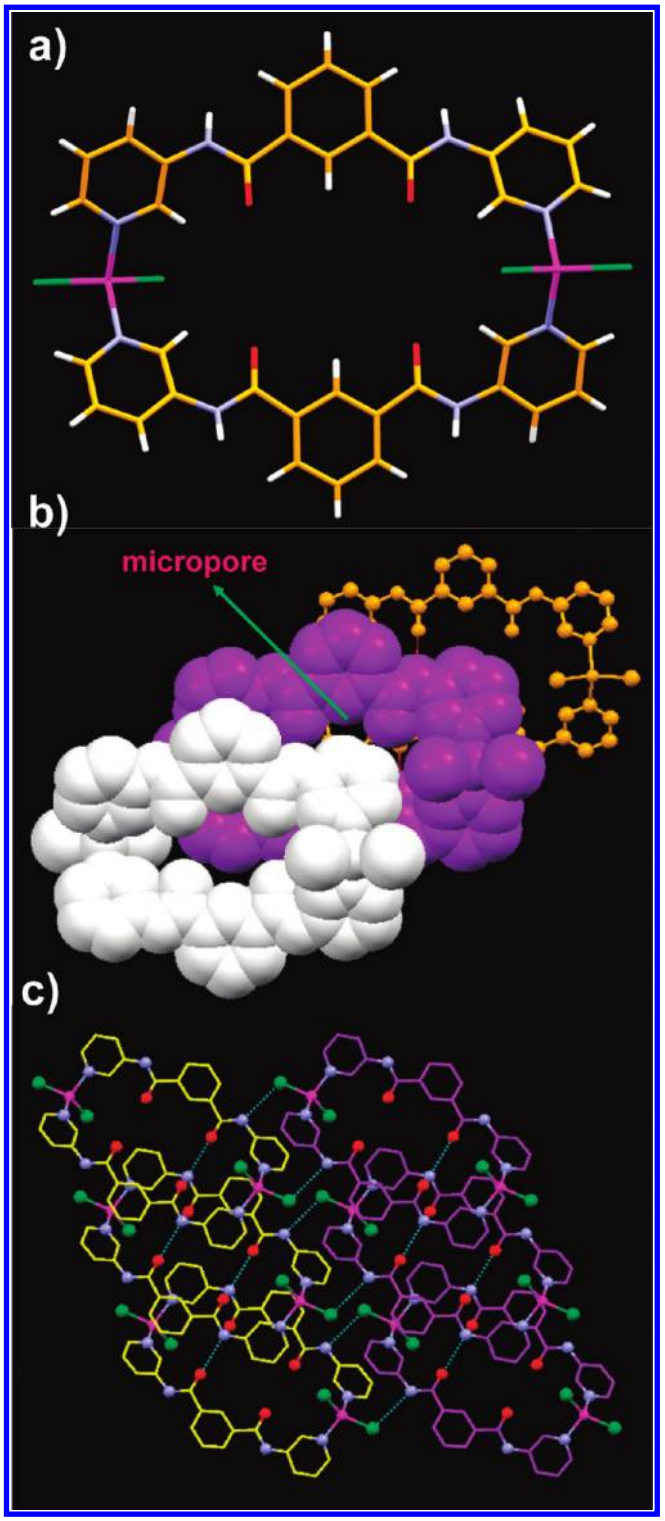

Figure 3. Crystal structure illustration of **1**; (a) metallamacrocycle; (b) 1-D hydrogen bonded chain of the metallamacrocycles sustained by N−H···O interactions; (c) parallel packing of the 1-D chains mediated by N−H···Cl interactions.

corresponding ligands and the metal salts under a similar solvent system used for gelation; the only difference we adopted was to use aq. EtOH in order to perform crystallization experiments following the layering method (see Experimental Section). For this purpose, we have slowly evaporated a diluted solution containing the various Zn^{II} halide salts separately with **L1** and **L2** in a 1:1 molar ratio that resulted in seven single crystals, namely, [{$Zn_2(\mu$-**L1**$)_2Cl_4$}] **1**, [{$Zn_2(\mu$-**L1**$)_2Br_4$}] **2**, [{$Zn_2(\mu$-**L1**$)_2I_4$}] **3**, [{Zn(μ-**L1**)Cl_2}·$2H_2O]_\infty$ **4**, and [{$Zn(X)_2(\mu$-**L2**)}.1/2EG]$_\infty$ **5**−**7** (where X = Cl for **5**, Br for **6**, and I for **7**).

When **L1** was reacted with $ZnCl_2$, $ZnBr_2$, and ZnI_2 separately in an aqueous DMF-aq·EtOH mixture, crystalline compounds **1**−**3** were isolated (see Experimental Section). Single crystal X-ray diffraction experimental analysis revealed that **1**−**3** were isomorphous crystals and belonged to the centrosymmetric triclinic $P\bar{1}$ space group (Table 1). The asymmetric unit was comprised of one Zn^{II}, a molecule of **L1**, and two halide anions (all coordinated to the metal center). The crystal structure can be best described as a bimetallic metallamacrocycle formed by coordinating two Zn^{II} metal centers by two ligands which were in *syn-syn-syn* conformation (Scheme S1, Supporting Information). The Zn^{II} metal center in **1**−**3** was significantly distorted from tetrahedral geometry as revealed from the corresponding ∠N−Zn−X, ∠N−Zn−N, and ∠X−Zn−X angles [where X = Cl, Br, and I, Table 3]. Interestingly, the metallamacrocycle present in these crystal structures has an oval shaped pore [2.963−3.147 × 7.99−8.23 by taking van der Waals radii in account] wherein all the amide carbonyls were pointed inward. The metallamacrocycles were further packed on top of each other in an offset fashion mediated by self-complementary *amide*−*amide* hydrogen bonding interactions [N(18)···O(9) = 2.982(4)−3.05(2) Å; ∠N(18)−H(18)···O(9) = 161.5−162.2°] resulting in an 1-D array and such offset packing prevented the guest molecules to be occluded within the macrocyclic pores. Such 1-D hydrogen bonded networks were further self-assembled via N−H···X interaction [N(7)···Cl(1) = 3.4278(19) Å, ∠N(7)−H(7)···Cl(1) = 153.5° in **1**; N(7)···Br(1) = 3.557(3) Å, ∠N(7)−H(7)···Br(1) = 153.7° in **2** and N(7)···I(1) = 3.828(13) Å, ∠N(7)−H(7)···I(1) = 155.0° in **3**] (Figure 3).

On the other hand, when **L1** was reacted with $ZnCl_2$ in ethylene glycol−aq. EtOH, crystals of a coordination polymer [{Zn(μ-**L1**)Cl_2}·$2H_2O]_\infty$ **4** was isolated after one week (see Experimental Section). Compound **4** was crystallized in the centrosymmetric monoclinic space group $P2_1/c$ (Table 2). The asymmetric unit was comprised of one Zn^{II}, one molecule of **L1**, two chloride anion (all coordinated to the metal center), and two molecules of water of solvation. The Zn^{II} metal center in **4** was significantly distorted from tetrahedral geometry as revealed from the corresponding ∠N−Zn−Cl, ∠N−Zn−N, and ∠Cl−Zn−Cl angles (Table 3). The extended coordination of ligand **L1** with Zn^{II} leads to the formation of a helical coordination polymer. Interestingly, the ligand **L1** retained its *syn-syn-syn* conformation in this structure, but rotation of the one of the pyridyl ring approximately 60.5° with respect to the central aromatic ring provided the required twist for the formation of helical coordination polymeric chains. Both left-handed and right-handed helical chains were found to pack in antiparallel fashion sustained by $\pi-\pi$ stacking (3.886(12) Å) interactions. The lattice included water molecules were located within the helical channel and were involved in hydrogen bonding with themselves [O(25)···O(26) = 2.76(2) Å], with the amide O = C [O(9)···O(25) = 2.731(18) Å] and amide N−H [N(7)···O(26) = 2.84(2)Å, ∠N(7)−H(7)···O(26) = 167.9°] of the adjacent helix (Figure 4). The thermogravimetric (TG) data also supported the presence of water molecules in the crystal lattice. TG showed a weight loss of 7.2%, which may be attributed to the loss of two solvated water molecules

Table 2. Crystal Data

crystal parameters	**1**	**2**	**3**	**4**	**5**	**6**
empirical formula	$C_{36}H_{28}Cl_4N_8O_4Zn_2$	$C_{36}H_{28}Br_4N_8O_4Zn_2$	$C_{36}H_{28}I_4N_8O_4Zn_2$	$C_{18}H_{18}Cl_2N_4O_4Zn$	$C_{19}H_{17}Cl_2N_4O_3Zn$	$C_{19}H_{17}Br_2N_4O_3Zn$
formula weight	909.20	1087.04	1275.00	490.63	485.64	574.56
crystal size/mm	0.32 × 0.28 × 0.16	0.24 × 0.18 × 0.12	0.16 × 0.12 × 0.08	0.24 × 0.18 × 0.12	0.18 × 0.12 × 0.06	0.28 × 0.22 × 0.12
crystal system	triclinic	triclinic	triclinic	monoclinic	triclinic	triclinic
space group	$P\bar{1}$	$P\bar{1}$	$P\bar{1}$	$P2_1/c$	$P\bar{1}$	$P\bar{1}$
a/Å	7.8015(6)	7.8225(9)	7.9309(16)	16.352(4)	8.671(11)	8.7547(3)
b/Å	8.4145(7)	8.4218(9)	8.821(2)	7.805(2)	9.631(13)	9.6918(4)
c/Å	14.7590(11)	14.8851(16)	15.170(3)	17.651(5)	13.505(17)	13.6550(5)
$\alpha/^0$	82.5080(10)	82.023(2)	83.763(11)	90.00	74.014(15)	73.3320(10)
$\beta/^0$	79.9360(10)	80.663(2)	81.709(11)	113.737(5)	74.102(16)	74.5630(10)
$\gamma/^0$	77.7080(10)	78.460(2)	80.531(11)	90.00	68.061(15)	67.6700(10)
volume/Å^3	927.71(13)	942.32(18)	1031.9(4)	2062.1(9)	987(2)	1010.41(7)
Z	1	1	1	4	2	2
$F(000)$	460	532	604	1000	494	566
μ MoKα /mm^{-1}	1.633	5.565	4.202	1.482	1.544	5.199
temperature/K	298(2)	298(2)	298(2)	298(2)	298(2)	298(2)
R_{int}	0.0203	0.0436	0.0268	0.0553	0.0867	0.0353
range of h, k, l	−9/9, −10/10, −17/17	−9/9, −9/10, −17/17	−8/8, −5/9, −16/15	−16/16, −7/7, −18/18	−8/8, −9/9, −13/13	−10/10, −11/11, −16/16
θ min/max/°	1.41/25.00	1.39/25.00	1.36/22.50	1.36/21.32	1.60/20.90	1.58/25.00
reflections collected/ unique/observed [$I > 2\sigma(I)$]	8912/3257/2936	9013/3306/2716	3565/2596/2050	12881/2297/1953	5985/2069/1603	9559/3554/2966
data/restraints/ parameters	3257/0/244	3306/0/244	2596/0/229	2297/0/262	2069/2/252	3554/0/263
goodness of fit on F^2	1.038	1.035	1.058	1.222	1.070	1.048
final R indices [$I > 2\sigma(I)$]	R_1 = 0.0270	R_1 = 0.0334	R_1 = 0.0660	R_1 = 0.0971	R_1 = 0.0813	R_1 = 0.0328
	wR_2 = 0.0768	wR_2 = 0.0761	wR_2 = 0.1812	wR_2 = 0.2899	wR_2 = 0.2237	wR_2 = 0.0785
R indices (all data)	R_1 = 0.0310	R_1 = 0.0448	R_1 = 0.0882	R_1 = 0.1061	R_1 = 0.0995	R_1 = 0.0430
	wR_2 = 0.0794	wR_2 = 0.0807	wR_2 = 0.2259	wR_2 = 0.2935	wR_2 = 0.2390	wR_2 = 0.0833

Table 3. Selected Bond Lengths (Å) and Bond Angles (°) Involving the Coordination Geometries of the Metal Centers

1			
Zn(1)−N(1)	2.0447(18)	N(1)−Zn(1)−N(23)	114.13(8)
Zn(1)−N(23)	2.0474(18)	N(1)−Zn(1)−Cl(2)	104.76(5)
Zn(1)−Cl(2)	2.2342(6)	N(23)−Zn(1)−Cl(2)	105.16(5)
Zn(1)−Cl(1)	2.2428(6)	N(1)−Zn(1)−Cl(1)	107.75(5)
		N(23)−Zn(1)−Cl(1)	106.92(5)
		Cl(2)−Zn(1)−Cl(1)	118.42(3)
2			
Zn(1)−N(1)	2.042(3)	N(1)−Zn(1)−N(23)	115.64(13)
Zn(1)−N(23)	2.045(3)	N(1)−Zn(1)−Br(2)	103.78(10)
Zn(1)−Br(2)	2.3763(7)	N(23)−Zn(1)−Br(2)	105.15(9)
Zn(1)−Br(1)	2.3783(6)	N(1)−Zn(1)−Br(1)	108.33(10)
		N(23)−Zn(1)−Br(1)	106.18(9)
		Br(2)−Zn(1)−Br(1)	118.19(3)
3			
Zn(1)−N(1)	2.059(13)	N(1)−Zn(1)−N(23)	113.0(6)
Zn(1)−N(23)	2.072(13)	N(1)−Zn(1)−I(2)	104.8(4)
Zn(1)−I(2)	2.568(2)	N(23)−Zn(1)−I(2)	106.9(4)
Zn(1)−I(1)	2.570(2)	N(1)−Zn(1)−I(1)	108.5(4)
		N(23)−Zn(1)−I(1)	105.9(4)
		I(2)−Zn(1)−I(1)	117.93(9)
4			
Zn(1)−N(1)	2.019(14)	N(1)−Zn(1)−N(23)	107.8(5)
Zn(1)−N(23)	2.054(15)	N(1)−Zn(1)−Cl(2)	108.5(5)
Zn(1)−Cl(2)	2.235(5)	N(23)−Zn(1)−Cl(2)	104.5(4)
Zn(1)−Cl(1)	2.246(5)	N(1)−Zn(1)−Cl(1)	110.4(4)
		N(23)−Zn(1)−Cl(1)	105.5(4)
		Cl(2)−Zn(1)−Cl(1)	119.4(2)
5			
Zn(1)−N(23)	2.036(10)	N(23)−Zn(1)−N(1)	102.5(4)
Zn(1)−N(1)	2.054(9)	N(23)−Zn(1)−Cl(2)	108.6(3)
Zn(1)−Cl(2)	2.208(4)	N(1)−Zn(1)−Cl(2)	109.7(3)
Zn(1)−Cl(1)	2.231(4)	N(23)−Zn(1)−Cl(1)	107.4(3)
		N(1)−Zn(1)−Cl(1)	105.1(3)
		Cl(2)−Zn(1)−Cl(1)	121.85(14)
6			
Zn(1)−N(1)	2.049(3)	N(1)−Zn(1)−N(23)	102.91(13)
Zn(1)−N(23)	2.051(3)	N(1)−Zn(1)−Br(2)	109.01(9)
Zn(1)−Br(2)	2.3527(6)	N(23)−Zn(1)−Br(2)	108.87(9)
Zn(1)−Br(1)	2.3743(6)	N(1)−Zn(1)−Br(1)	105.55(9)
		N(23)−Zn(1)−Br(1)	107.20(9)
		Br(2)−Zn(1)−Br(1)	121.70(2)

(calc. weight loss = 7.4%) within the temperature range of 27−277 °C (Figure S5, Supporting Information).

PXRD comparison plots revealed that none of the xerogels of **G1**, **G2**, and **G3** showed any match with the corresponding simulated PXRD patterns derived from the single crystal data of **1**, **2**, and **3**, respectively (Figure S1, Supporting Information); this means that coordination compounds responsible for the gel network formation of **G1**−**G3** were not made from the corresponding metallmacrocycles **1**−**3**, respectively. Interestingly, the PXRD pattern of xerogel of **G1** matched quite well with that of the simulated and bulk PXRD patterns of the helical coordination polymer **4** (Figure 5a). PXRD patterns of the xerogels of **G2** and **G3** showed close resemblance with that of the simulated pattern of **4** (Figures S2 and S3, Supporting Information). Since the change in **G2** and **G3** is in the corresponding anion (Br for **G2** and I for **G3**), the close resemblance of the PXRD patterns of these xerogels with that of **4** might be due to isomorphism, meaning that a similar helical structure as observed in **4** may be responsible for the gel network formation in **G2** and **G3**. However, in the absence of single crystal structures of the isomorphous crystals having helical topology with bromide and iodide as counteranions (if there are any), it is difficult to come to such conclusion with certainty.

The ligand **L2** did not react with ZnX_2 (where X = Cl, Br and I) in an aq. DMF−EtOH mixture; only the crystals of **L2** were obtained. However, by changing the solvent system to ethylene glycol−aq. EtOH, block shaped crystals of $[\{Zn(Cl)_2(\mathbf{L2})\}\cdot 1/2EG]_\infty$ **5**, $[\{Zn(Br)_2(\mathbf{L2})\}\cdot 1/2EG]_\infty$ **6**, and $[\{Zn(I)_2(\mathbf{L2})\}\cdot 1/2EG]_\infty$ **7** were isolated (see Experimental Section). While the structures of **5** and **6** were established using single crystal X-ray diffraction (vide infra), the chemical formula of **7** was established based on elemental analysis, FT-IR, and PXRD (see Experimental Section).

Crystals of **5**−**6** were found to be isomorphous; they were crystallized in the centrosymmetric triclinic space group $P\bar{1}$

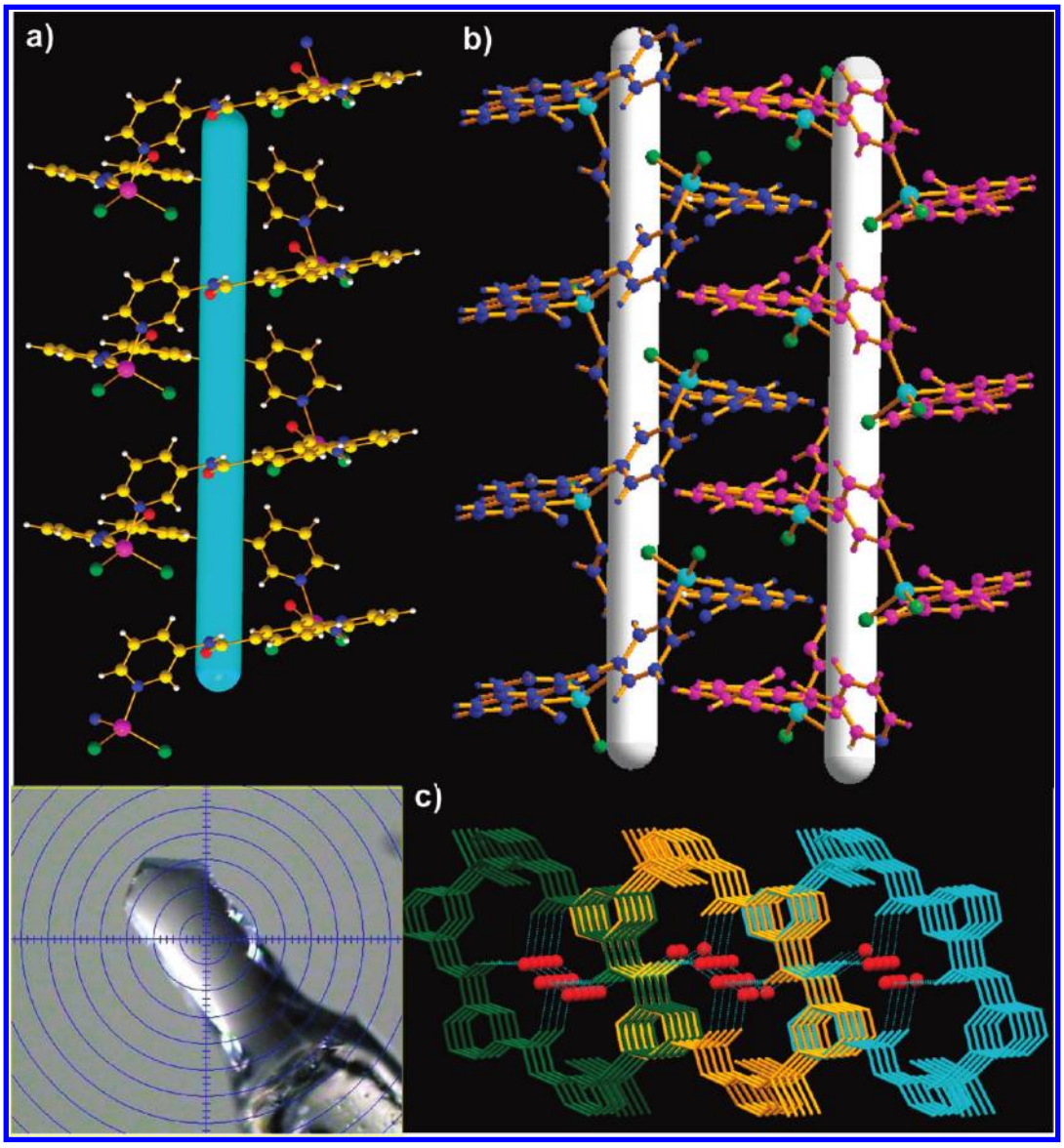

Figure 4. Crystal structure illustration of **4**; (a) 1-D right-handed helical coordination polymer; (b) parallel arrangement of two helical chains of opposite handedness; (c) arrangement of helical chains viewed from the top displaying location of solvate water molecules (red balls) within the helix channels (inset − the photograph of the single crystal of **4** used for data collection).

(Table 2). The asymmetric unit was comprised of one Zn^{II}, a molecule of **L1**, and two Cl^-/Br^- anions (all coordinated to the metal center) and a half a molecule of ethylene glycol which was located around the center of inversion. The crystal structure can be described as a 1D zigzag coordination polymer arising due to the extended coordination of **L2** in its *syn-anti-anti* conformation (Scheme S2, Supporting Information) with Zn^{II}. The metal centers in these structures **5**−**6** were significantly distorted from tetrahedral geometry as revealed from the corresponding ∠N−Zn−Cl^-/Br^-, ∠N−Zn−N, and ∠Cl^-/Br^-−Zn−Cl^-/Br^- angles (Table 3). Interestingly, the zigzag coordination polymer interacts with the guest ethylene glycol molecule mediated by hydrogen bonding of amide C═O [O···O = 2.78(2)−2.844(6) Å, ∠O−H···O = 164.3°] and amide N−H [N(7)···O(25) = 2.92(2)−2.925(7) Å]. Moreover, amide N−H is also involved in hydrogen bonding with metal bound chloride and bromide anions in **5** and **6**, respectively [N···Cl = 3.502(10) Å; ∠N−H···Cl = 164.8° and N···Br = 3.607(3) Å; ∠N−H···Br = 166.2°] (Figure 6). The TG data of the crystals of **5** and **6** also further supported these findings. Both **5** and **6** showed a weight loss of 5.4% and 5.6%, which may be attributed to the loss of 0.5 solvated EG molecules (calc. weight loss for 0.5 EG = 6.4% for **5** and 5.4% for **6**) within the temperature range of 27−122 °C and 21−127 °C, respectively (Figures S6−S7, Supporting Information).

The PXRD patterns of the xerogels of **G7**−**G9** could not be compared with any simulated pattern in the absence of single crystal structures of the corresponding coordination compounds. However, the chemical formulas of these xerogels were established as $[\{Zn(\mathbf{L2})Cl_2\}\cdot 4H_2O]_\infty$ (**G7**), $[\{Zn(\mathbf{L2})Br_2\}\cdot 4H_2O]_\infty$ (**G8**), and $[\{Zn(\mathbf{L2})I_2\}\cdot 3H_2O]_\infty$ (**G9**) based on FT-IR and elemental analysis data (Supporting Information); insolubility of these xerogels in common solvents also supported the coordination polymeric nature of these compounds.

PXRD pattern of the xerogels of **G10** and **G11** showed nearly identical resemblance with that of the corresponding bulk solid of **5** and **6**, respectively; however, the simulated pattern of both **5** and **6** did not match quite well with the corresponding bulk and xerogel patterns indicating the presence of other crystalline morph (Figure 5b,c).

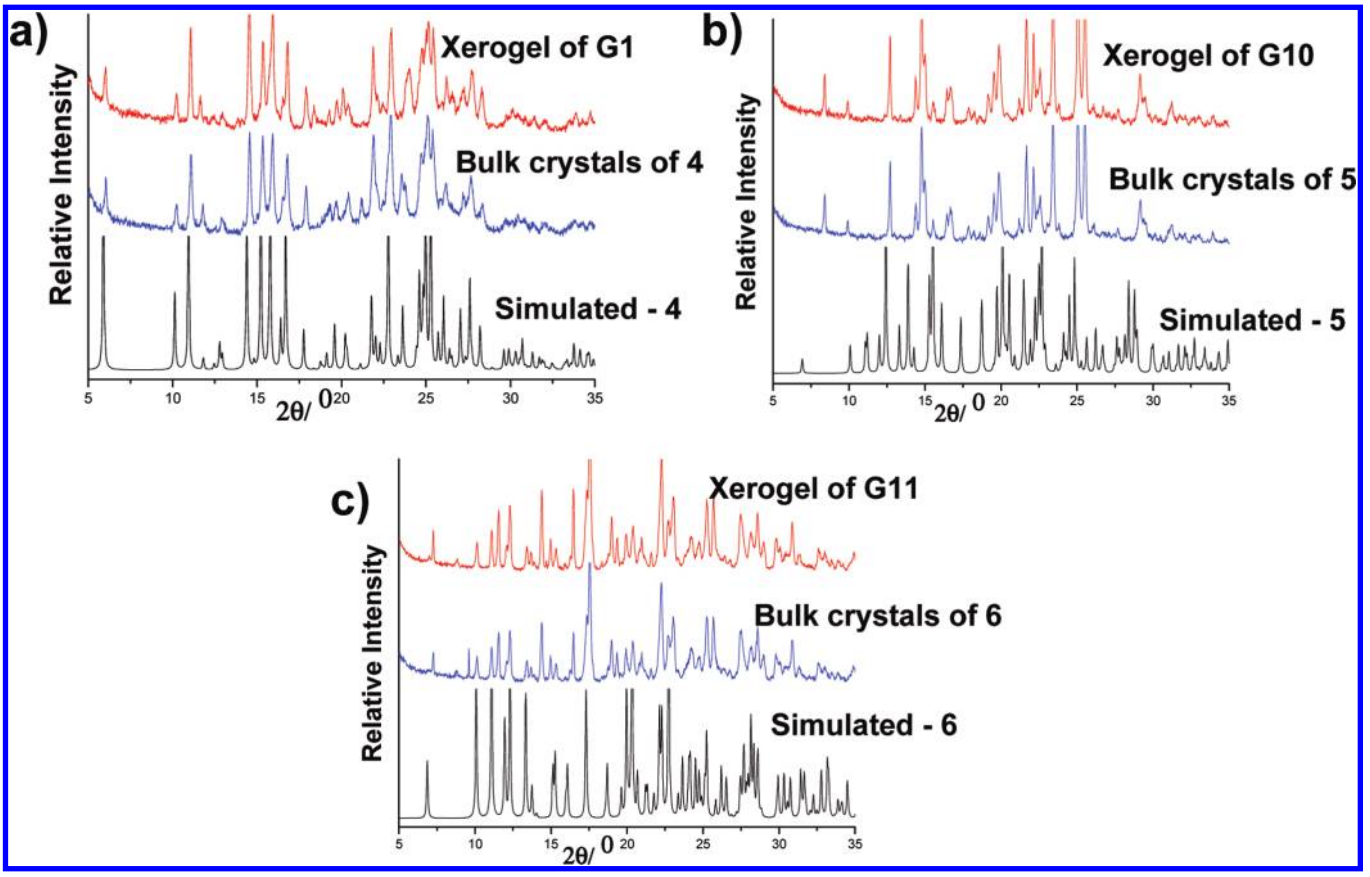

Figure 5. (a−c) PXRD comparison plots of **1**, **5**, and **6** under various conditions.

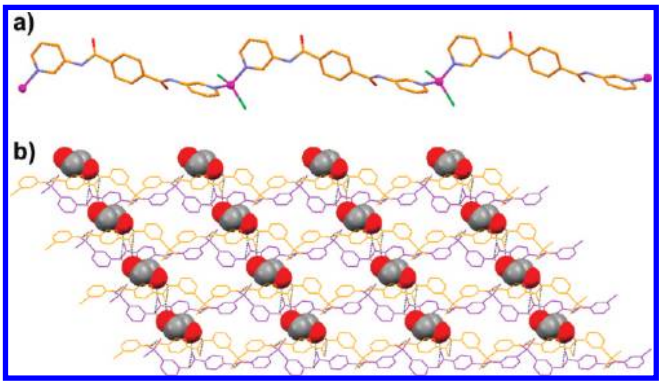

Figure 6. Crystal structure illustration of **5**; (a) 1D zigzag coordination polymer; (b) the entrapment of ethylene glycol within the interstitial space of the coordination polymer.

The PXRD patterns of the xerogel of **G12** displayed an excellent match with that of the crystals of **7**. These patterns in turn showed a reasonable match with that of the simulated PXRD pattern of **6**, indicating that crystals of **7** and xerogel of **G12** were crystallographically identical and most likely isomorphous with **6** (Figure S4, Supporting Information). However, in the absence of the single crystal structure of **7**, it is not possible to conclude with certainty.

To get a clearer picture, we have summarized the results in Table 4. Both solvent system and concentration play a crucial role in the outcome of the experiments; at relatively high concentration (4−10 wt %), gels were formed in DMF/water, and EG/water. EtOH as well as a relatively lower concentration seem to have played a crucial in getting X-ray quality crystals in most of the cases. It is interesting to note that **L2** did not react with the metal salts in DMF/water/EtOH leaving the ligand **L2** crystallized out. On the basis the PXRD and SXRD data, it may be reasonable to conclude (although not with full certainty) that all the gel networks were most likely comprised of 1-D network, that is, either helix (**G1**−**G3**) or zigzag coordination polymers (**G10**−**G12**). Most interestingly, SXRD data clearly established that the gel forming network such as helix and zigzag were all solvated, which supported the hypothesis based on which present studies were carried out.

Conclusion

Thus, we have discovered a new series of metallogelators derived from the bidentate hydrogen bond equipped bis-pyridyl-bis-amide ligands **L1** and **L2**, and Zn^{II} halides. It is clear from the results that solvent and concentration of the reaction mixture play a crucial role in gelation and crystallization. While the structure of the gel network in the xerogel of **G1** is established as helical coordination polymer **4**, the structures of the gel network in the xerogels of **G10** and **G11** are most likely to be the zigzag coordination polymers **5** and **6**, respectively, as revealed by the SXRD and PXRD data. Similarly, the structures of the gel network in the xerogels of **G2**−**G3**, and **G12** appear to be the helical and zigzag coordination polymer as in **4** and **6**, respectively. Moreover, the crystal structures of **4** (helical), **5** and **6** (both 1-D zigzag) reveal the presence lattice included solvent (water/ethylene glycol),which support the hypothesis based on which designs of these metallogelators are inspired. The fact that the metallamacrocycle **1**, **2**, and **3** did not show any lattice included solvents as well as metallogelation properties reinforce the proof of the concept further.

Table 4. Summary of the Overall Results

	L1				L2			
	DMF/water (0.3:0.7)	DMF/water/ EtOH (3:8:7)	EG/water (0.3:0.7)	EG/water/ EtOH (4:1:4)	DMF/water (0.3:0.7)	DMF/water/ EtOH (3:8:7)	EG/water (0.3:0.7)	EG/water/ EtOH (4:1:4)
$ZnCl_2$	**G1** = **4** (helix) 4.3 wt %[a] (PXRD, SXRD)	**1** (macrocycle) 3.2 wt %[b] (SXRD)	**P4** = **4**(helix) (PXRD, SXRD)	**4** (helix) 3.2 wt %[b] (SXRD)	**G7** 7.2 wt %[a] (unknown)	**L2** 3.2 wt %[b] (PXRD)	**G10~5** (zigzag) 4.3 wt %[a] (PXRD)	**5** (zigzag) 3.2 wt %[b] (SXRD)
$ZnBr_2$	**G2~4** (helix) 5.1 wt %[a] (PXRD, SXRD)	**2** (macrocycle) 3.7 wt %[b] (SXRD)	**P5** (unknown)	**2** (macrocycle) 3.7 wt %[b] (PXRD, SXRD)	**G8** 8.6 wt %[a] (unknown)	**L2** 3.7 wt %[b] (PXRD)	**G11~6** (zigzag) 5.1 wt %[a] (PXRD)	**6** (zigzag) 3.7 wt %[b] (SXRD)
ZnI_2	**G3~4** (helix) 6.0 wt %[a] (PXRD, SXRD)	**3** (macrocycle) 4.4 wt %[b] (SXRD)	**P6** (unknown)	**3** (macrocycle) 4.4 wt %[b] (PXRD, SXRD)	**G9** 10.0 wt %[a] (unknown)	**L2** 4.4 wt %[b] (PXRD)	(**G12** = **7**)~**6** (zigzag) 6.0 wt %[a] (PXRD)	**7**~**6** (zigzag) 4.4 wt %[b] (PXRD)

[a] Concentration required to get gel. [b] Concentration required to get a single crystal; PXRD and SXRD within the parentheses indicate the physicochemical techniques used to establish the structural identity.

Experimental Section

Materials and Methods. All chemicals were commercially available (Aldrich) and used without further purification. While the ligand *N, N′*-bis-(3-pyridyl)isophthalamide **L1** was synthesized by following a reported procedure,[21] *N,N′*-bis-(3-pyridyl)terephthalamide **L2** was previously reported by us.[15e] The elemental analysis was carried out using a Perkin-Elmer 2400 Series-II CHN analyzer. FT-IR spectra were recorded using Perkin-Elmer Spectrum GX, and TGA analyses were performed on a SDT Q Series 600 Universal VA.2E TA Instruments. X-ray powder diffraction patterns were recorded on a Bruker AXS D8 Advance Powder (Cu $K_{\alpha 1}$ radiation, $\lambda = 1.5406$ Å) X-ray diffractometer. Scanning electron microscopy (SEM) was recorded in a JEOL, JMS-6700F, field emission scanning electron microscope. Rheology experiments were performed in SDT Q Series Advanced rheometer AR 2000.

Synthesis of the Coordination Compounds 1−7. 1−3 were synthesized by layering a DMF-EtOH (1:3 v/v) solution of **L1** (40 mg, 0.128 mmol) over aqueous solution of $ZnCl_2$ (17.5 mg, 0.128 mmol), $ZnBr_2$ (28.5 mg, 0.128 mmol), and ZnI_2 (41 mg, 0.128 mmol), respectively. After two weeks, X-ray quality crystals were obtained by a slow evaporation technique.

1: Yield: 35.0% (40 mg, 0.044 mmol). Anal. data calc. for $C_{36}H_{28}N_8O_4Zn_2Cl_4$: C, 47.55; H, 3.10; N, 12.32. Found: C, 47.74; H, 3.39; N, 12.65. FT-IR (KBr, cm^{-1}): 3323 (s, N−H stretch), 3070 (m, aromatic C−H stretch), 1681 and 1658 (s, amide C=O stretch), 1612 (s, amide C=O bend), 1583s, 1543s, 1529s, 1481s, 1423s, 1330s, 1292s, 1274s, 1240s, 1193m, 1124m, 1057s, 953m, 812s, 725s, 696s, 684s, 650s, 609s, 594s cm^{-1}.

2: Yield: 35.0% (50 mg, 0.046 mmol). Anal. data calc. for $C_{36}H_{28}N_8O_4Zn_2Br_4$: C, 39.78; H, 2.60; N, 10.31. Found: C, 39.76; H, 2.42; N, 9.85. FT-IR (KBr, cm^{-1}): 3325 (s, N−H stretch), 3115, 3018 (s, aromatic C−H stretch), 1681 and 1658 (s, amide C=O stretch), 1610 (s, amide C=O bend), 1581s, 1545s, 1529s, 1479s, 1425s, 1325w, 1332s, 1292s, 1274s, 1240s, 1192m, 1178w, 1130s, 1103s, 1057s, 935m, 896m, 879m, 842w, 812s, 725s, 696s, 684s, 669m, 650s, 609s, 588s, 530m, 501m, 412s cm^{-1}.

3: Yield: 37.0% (60 mg, 0.047 mmol). Anal. data calc. for $C_{36}H_{28}N_8O_4Zn_2I_4$: C, 33.91; H, 2.21; N, 8.79. Found: C, 34.12; H, 2.20; N, 8.88. FT-IR (KBr, cm^{-1}): 3331 (s, N−H stretch), 3221 (s, aromatic C−H stretch), 1681 and 1658 (s, amide C=O stretch), 1610 (s, amide C=O bend), 1581s, 1541s, 1525s, 1479s, 1423s, 1352s, 1290s, 1274s, 1238s, 1192 m, 1178 m, 1132s, 1103s, 1057s, 935 m, 916 m, 810s, 723s, 696s, 682s, 648s, 609s, 594s, 574w, 501w cm^{-1}.

4 was synthesized by layering aqueous methanolic solution of $ZnCl_2$ (17.5 mg, 0.128 mmol) over ethylene glycol solution of **L1** (40 mg, 0.128 mmol). After one week X-ray quality crystals were obtained. Yield: 64% (40 mg, 0.08 mmol). Anal. data calc. for $C_{18}H_{14}N_4O_2ZnCl_2.2H_2O$: C, 44.06; H, 3.70; N, 11.42. Found: C, 43.84; H, 3.50; N, 11.65. FT-IR (KBr, cm^{-1}): 3323 (s, N−H stretch), 3219 (s, aromatic C−H stretch), 1681 and 1658 (s, amide C=O stretch), 1612 (s, amide C=O bend), 1581s, 1543s, 1529s, 1479s, 1423s, 1352m, 1330s, 1292s, 1274s, 1240s, 1193 m, 1176 m, 1124s, 1101s, 1057s, 935m, 810s, 723s, 696s, 684s, 650s, 609s, 594s, 524w, 501w, 480w cm^{-1}.

5 and **6** were synthesized by layering an aqueous ethanolic solution of $ZnCl_2$ (17.5 mg, 0.128 mmol) and $ZnBr_2$ (28.5 mg, 0.128 mmol) respectively over an ethylene glycol solution of **L2** (40 mg, 0.128 mmol). After one week, X-ray quality crystals of **5** and **6** and thin plate shaped crystals of **7** were obtained.

5: Yield: 65% (40 mg, 0.08 mmol). Anal. data calc. for $C_{18}H_{14}N_4O_2ZnCl_2 \cdot 1/2EG$: C, 46.99; H, 3.53; N, 11.51. Found: C, 46.12; H, 3.46; N, 11.20. FT-IR (KBr, cm^{-1}): 3317 (s, N−H stretch), 3064 (s, aromatic C−H stretch), 1677 (s, amide C=O stretch), 1610 (s, amide C=O bend), 1585s, 1535s, 1485s, 1423s, 1330s, 1290s, 1244s, 1191s, 1126s, 1108s, 1043m, 1020m, 887m, 850m, 808s, 694s, 651s, 609w cm^{-1}.

6: Yield: 65% (40 mg, 0.08 mmol). Anal. data calc. for $C_{18}H_{14}N_4O_2ZnBr_2 \cdot 1/2EG$: C, 39.72; H, 2.98; N, 9.75. Found: C, 39.92; H, 3.31; N, 9.62. FT-IR (KBr, cm^{-1}): 3317 (s, N−H stretch), 3064 (s, aromatic C−H stretch), 1677 (s, amide C=O stretch), 1610 (s, amide C=O bend), 1585s, 1535s, 1485s, 1423s, 1330s, 1290s, 1244s, 1191s, 1126s, 1108s, 1043m, 1020m, 887m, 850m, 808s, 694s, 651s, 609w cm^{-1}.

7: Yield: 68% (50 mg, 0.09 mmol). Anal. data calc. for $C_{18}H_{14}N_4O_2ZnI_2 \cdot 1/2EG$: C, 34.13; H, 2.56; N, 8.38. Found: C, 34.02; H,

2.99; N, 8.56. FT-IR (KBr, cm^{-1}): 3336 (s, ethylene glycol O−H stretch), 3058 (s, N−H stretch), 2921 (s, aromatic C−H stretch), 2852s, 1681 (s, amide C═O stretch), 1612 (s, amide C═O bend), 1587s, 1527s, 1487s, 1423s, 1332s, 1290s, 1272s, 1247s, 1195s, 1107s, 1062m, 1016m, 804s, 719s, 694s, 653s, 613m, 568s cm^{-1}.

Single Crystal X-ray Diffraction. Single crystal X-ray data were collected using Mo Kα (λ = 0.7107 Å) radiation on a SMART APEX II diffractometer equipped with CCD area detector. Data collection, data reduction, structure solution/refinement were carried out using the software package of SMART APEX II. All structures were solved by direct method and refined in a routine manner. In most of the cases, non-hydrogen atoms were treated anisotropically. Hydrogen atom positions were generated by their idealized geometry and refined using a riding model.

Acknowledgment. We thank Department of Science & Technology (DST), New Delhi, India, for financial support. A.N.N. thanks IACS for a Senior Research Fellowship. Single crystal X-ray diffraction data were collected at CSMCRI, Bhavnagar (paid service) and the DST-funded National Single Crystal Diffractometer Facility at the Department of Inorganic Chemistry, IACS.

Supporting Information Available: Molecular plots and hydrogen bonding parameters for **1**−**6**, Schemes S1 and S2, Figures S1−S4, thermogravimetric analysis data (Figures S5−S7), and crystallographic data in CIF format. This material is available free of charge via the Internet at http://pubs.acs.org.

References

(1) Menger, F. M.; Caran, K. L. *J. Am. Chem. Soc.* **2000**, *122*, 11679.
(2) (a) Terech, P.; Weiss, R. G. *Chem. Rev.* **1997**, *97*, 3133. (b) Abdallah, D. J.; Weiss, R. G. *Adv. Mater.* **2000**, *12*, 1237. (c) Dastidar, P. *Chem. Soc. Rev.* **2008**, *37*, 2699. (d) George, M.; Weiss, R. G. *Acc. Chem. Res.* **2006**, *39*, 489. (e) Sangeetha, N. M.; Maitra, U. *Chem. Soc. Rev.* **2005**, *34*, 821. (f) Pal, A.; Basit, H.; Sen, S.; Aswal, V. K.; Bhattacharya, S. *J. Mater. Chem.* **2009**, *19*, 4325. (g) Ajayaghosh, A.; Praveen, V. K. *Acc. Chem. Res.* **2007**, *40*, 644. (h) Estroff, L. A.; Hamilton, A. D. *Chem. Rev.* **2004**, *104*, 1201. (i) Steed, J. W. *Chem. Soc. Rev.* **2010**, *39*, 3686. (j) Smith, D. K. *Adv. Mater.* **2006**, *18*, 2773.
(3) (a) Piepenbrock, M.-O. M.; Lloyd, G. O.; Clarke, N.; Steed, J. W. *Chem. Rev.* **2010**, *110*, 1960. (b) Fages, F. *Angew. Chem., Int. Ed.* **2006**, *45*, 1680.
(4) Xing, B.; Choi, M.-F.; Xu, B. *Chem. Commun.* **2002**, 362.
(5) (a) Lopez, D.; Guenet, J.-M. *Macromolecules* **2001**, *34*, 1076. (b) Terech, P.; Gebel, G.; Ramasseul, R. *Langmuir* **1996**, *12*, 4321. (c) Ishi-I, T.; Iguchi, R.; Snip, E.; Ikeda, M.; Shinkai, S. *Langmuir* **2001**, *17*, 5825. (d) Kimura, M.; Muto, T.; Takimoto, H.; Wada, K.; Ohta, K.; Hanabusa, K.; Shirai, H.; Kobayashi, N. *Langmuir* **2000**, *16*, 2078.
(6) Terech, P.; Schaffhauser, V.; Maldivi, P.; Guenet, J. M. *Langmuir* **1992**, *8*, 2104.
(7) Hanabusa, K.; Maesaka, Y.; Suzuki, M.; Kimura, M.; Shirai, H. *Chem. Lett.* **2000**, 1168.
(8) (a) Coates, I. A.; Smith, D. K. *J. Mater. Chem.* **2010**, *20*, 6696. (b) Bhattacharya, S.; Srivastava, A.; Pal, A. *Angew. Chem., Int. Ed.* **2006**, *45*, 2934. (c) Basit, H.; Pal, A.; Sen, S.; Bhattacharya, S. *Chem.−Eur. J.* **2008**, *14*, 6534. (d) Bose, P. P.; Drew, M. G. B.; Banerjee, A. *Org. Lett.* **2007**, *9*, 2489. (e) Vemula, P. K.; Aslam, U.; Mallia, V. A.; John, G. *Chem. Mater.* **2007**, *19*, 138.
(9) (a) Batabyal, S. K.; Leong, W. L.; Vittal, J. J. *Langmuir* **2010**, *26*, 7464. (b) Piepenbrock, M.-O. M.; Clarke, N.; Steed, J. W. *Langmuir* **2009**, *25*, 8451. (c) Srivastava, A.; Ghorai, S.; Bhattacharjya, A.; Bhattacharya, S. *J. Org. Chem.* **2005**, *70*, 6574. (d) Sreenivasachary, N..; Lehn, J-M. *Proc. Natl. Acad. Sci. U. S. A.* **2005** *102*, 5938.
(10) (a) Escuder, B.; Miravet, J. F. *Chem. Commun.* **2005**, 5796. (b) Bull, S. R.; Guler, M. O.; Bras, R. E.; Meade, T. J.; Stupp, S. I. *Nano Lett.* **2005**, *5*, 1. (c) Kishimura, A.; Yamashita, T.; Yamaguchi, K.; Aida, T. *Nat. Mater.* **2005**, *4*, 546. (d) Roubeau, O.; Colin, A.; Schmitt, V.; Clérac, R. *Angew. Chem., Int. Ed.* **2004**, *43*, 3283.
(11) (a) Klawonn, T.; Gansäuer, A.; Winkler, I.; Lauterbach, T.; Franke, D.; Nolte, R. J. M.; Feiters, M. C.; Börner, H.; Hentschel, J.; Dötz, K. H. *Chem. Commun.* **2007**, 1894. (b) Tam, A. Y.-Y.; Wong, K. M.-C.; Yam, V. W.-W. *J. Am. Chem. Soc.* **2009**, *131*, 6253. (c) Yoon, S.; Kwon, W. J.; Piao, L.; Kim, S.-H. *Langmuir* **2007**, *23*, 8295. (d) Xing, B.; Choi, M.-F.; Xu, B. *Chem.—Eur. J.* **2002**, *8*, 5028. (e) Sahoo, P.; Kumar, D. K.; Trivedi, D. R.; Dastidar, P. *Tetrahedron Lett.* **2008**, *49*, 3052.
(12) (a) Kumar, D. K.; Jose, D. A.; Dastidar, P.; Das, A. *Chem. Mater.* **2004**, *16*, 2332. (b) Kumar, D. K.; Jose, D. A.; Das, A.; Dastidar, P. *Chem. Commun.* **2005**, 4059. (c) Adarsh, N. N.; Kumar, D. K.; Dastidar, P. *Tetrahedron* **2007**, *63*, 7386. For reviews on supramolecular synthons and crystal engineering see (d) Desiraju, G. R. *Crystal Engineering: The Design of Organic Solids*, Elsevier: Amsterdam, 1989. (e) Desiraju, G. R. *Angew. Chem., Int. Ed.* **1995**, *34*, 2311. (f) Desiraju, G. R. *Angew. Chem., Int. Ed.* **2007**, *46*, 8342.
(13) Lebel, O.; Perron, M.-E.; Maris, T.; Zalzal, S. F.; Nanci, A.; Wuest, J. D. *Chem. Mater.* **2006**, *18*, 3616.
(14) Adarsh, N. N.; Sahoo, P.; Dastidar, P. *Cryst. Growth Des.* **2010**, *10*, 4976.
(15) (a) Adarsh, N. N.; Tocher, D. A.; Ribas, J.; Dastidar, P. *New J. Chem.* **2010**, *34*, 2458. (b) Adarsh, N. N.; Kumar, D. K.; Dastidar, P. *CrystEngComm* **2009**, *11*, 796. (c) Yue, N. L. S.; Eisler, D. J.; Jennings, M. C.; Puddephatt, R. J. *Inorg. Chem.* **2004**, *43*, 7671. (d) Yue, N.; Qin, Z.; Jennings, M. C.; Eisler, D. J.; Puddephatt, R. J. *Inorg. Chem. Commun.* **2003**, *6*, 1269. (e) Adarsh, N. N.; Dastidar, P. *Cryst. Growth Des.* **2010**, *10*, 483.
(16) (a) Adarsh, N. N.; Kumar, D. K.; Dastidar, P. *Inorg. Chem. Commun.* **2008**, *11*, 636. (b) Qin, Z.; Jennings, M. C.; Puddephatt, R. J. *Chem.—Eur. J.* **2002**, *8*, 735. (c) Adarsh, N. N.; Kumar, D. K.; Suresh, E.; Dastidar, P. *Inorg. Chim. Acta* **2010**, *363*, 1367.
(17) (a) Adarsh, N. N.; Kumar, D. K.; Dastidar, P. *Cryst. Growth Des.* **2009**, *9*, 2979. (b) Kumar, D. K.; Das, A.; Dastidar, P. *CrystEngComm* **2006**, *8*, 805.
(18) Anderson, K. M.; Day, G. M.; Paterson, M. J.; Byrne, P.; Clarke, N.; Steed, J. W. *Angew. Chem., Int. Ed.* **2008**, *47*, 1058.
(19) Ostuni, E.; Kamaras, P.; Weiss, R. G. *Angew. Chem., Int. Ed.* **1996**, *35*, 1324.
(20) (a) Piepenbrock, M-O. M.; Clarke, N.; Steed, J. W. *Langmuir* **2009**, *25*, 8451. (b) Byrne, P.; Lloyd, G. O.; Applegarth, L.; Anderson, K. M.; Clarke, N.; Steed, J. W. *New. J. Chem.* **2010**, *34*, 2261. (c) Trivedi, D. R.; Dastidar, P. *Chem. Mater.* **2006**, *18*, 1470.
(21) Qin, Z.; Jennings, M. C.; Puddephatt, R. J. *Inorg. Chem.* **2003**, *42*, 1956.